

FLUTTER CALCULATIONS AND TRANSONIC WIND TUNNEL TESTING OF DYNAMICALLY SCALED MODEL OF THE HIGH-ASPECT-RATIO WING

Azarov Yu.A.*, **Liseykin G.V.***, **Pronin M.A.***, **Orlova O.A.***
***Central Aerohydrodynamic Institute (TsAGI), Zhukovsky, Russia**
Keywords: wind tunnel, dynamically scaled model, flutter

Abstract

Studies of aeroelasticity characteristics of dynamically scaled models are actual task. There is included computational research and experimental studies in wind tunnels. In this paper discussed experience of studies of high-aspect-ratio wing dynamically scaled model tested in transonic wind tunnel.

1 Computational research

The calculations were done for two mathematical models: one using spatial beam schematization and another using finite-element method (FEM).

Mathematical beam model of the dynamically scaled model of the wing is simply presented on the Fig 1. The spatial beams schematization lies at the heart of model: such structure parts as wing, wing attachment and aileron are modeled by the elastic beams, which have torsion rigidity GI_p and bending stiffness EI in two mutually perpendicular planes (EI_v at a bend in a vertical direction and EI_h – in horizontal). Beams bear the distributed masses m , with distance σ from a stiffness axis, and the distributed moments of inertia I_m . The model have suspended objects of different functions (remote engines and pylons), attached to beams. Beams are highlighted with black colors, aerodynamic surfaces are blue, concentrated masses such as engine and pylon are red colored. Every beam has different number of sections. Number of sections is selected to satisfy beam stiffnesses and inertial characteristics. The root wing beam is attached to the last section of attachment beam. Aileron

is also presented like beam for better accordance and attached to the terminal wing beam at appropriate section (at the same position like in full-scale model). A wing has the sweep angle χ , counted from corresponding axis of rigidity. Model haven't got sharp bend in dihedral angle as it was counted that it doesn't matter flutter behavior.

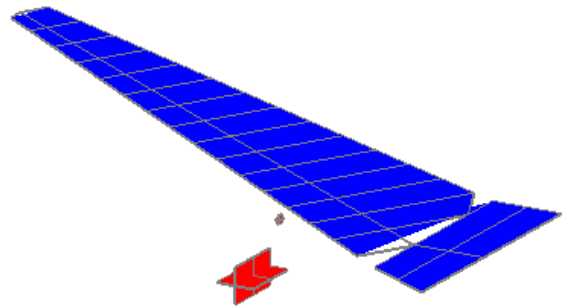


Fig 1. Beam model

Heavy objects represented by point masses with their inertial characteristics which are connected with root wing beam by an appropriate method. Also, attachment beam of the wing elastically connected to the "wall". From two considered objects, only engine under a wing have elastic attachment. Influence matrixes of engine were obtained from experiment. The influence matrix is considered regarding to the engine gravity centre. Its each element represents or linear displacement w (m) along an axis, specified in its index, or angular displacement ϑ (rad) about an axis, specified in its index, at application in the center gravity of unit force Q (kgf) in a direction specified in its index, or at application unit moment M (kgf*m) round an axis, specified in its index. In addition, according to the experiment measuring the static stiffness it was found that there is an influence between wing and solid attachment.

It was adjusted to agree with GVT experimental eigenmodes and eigenfrequencies.

Fig 2 shows finite-element (FE) model of wing of dynamically scaled model that was developed in software package MSC.Nastran.

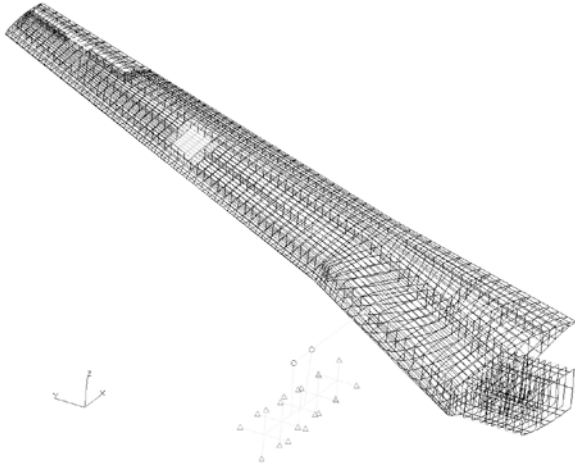


Fig 2. Finite-element model

Finite element model of the wing contains 228 BEAM-elements, 3982 QUAD-elements, 680 HEX-elements, 4 MPC-elements, 20 POINT-elements and 4160 nodes to satisfy full-scale design. Geometrical and mass characteristics were reconcile the geometrical and mass characteristics of nature experimental full-scale wing dynamically scaled model. Stiffness characteristics of FE model were slightly corrected to correspond Stiffness Tests and in the first place Ground Vibration Tests (GVT). Generally elastic characteristics of some materials were increased to satisfy Ground Vibration Tests.

Total inertial characteristics, eigen frequencies and eigen modes for beam model and FE model were calculated and then these results were compared with GVT tests results. Eigen modes and frequencies of beam model are defined by finding solution of the both integral and algebraic equations by a successive iterations method. Convergence of a method is approved by convergence of frequencies and amplitudes of forms in a number of chosen points.

Both models are in good agreement with the experimental data and relative error δ doesn't exceed 5% but there are also some

discrepancies. Fig 3 shows main difference in second mode form (pitch of engine). While in GVT and beam-model pitch of engine interacts with 1-st wing bending mode in FE model engine pitch interacts with wing torsion.

This difference is due to compliance in connection of the wing to attachment. In FE model MPC-connectors perform such compliance while in beam model compliance performed with influence matrix.

For the flutter calculation of FE model aerodynamic flutter model was performed in the software package MSC.FlightLoads. Aerodynamic model include two aerodynamic surfaces: 1) from the root of the wing to the sharp bend and 2) from sharp bend to the end of the wing. Additional aerodynamic surfaces were built for different types of wing tips. Structural node deformations of the upper skin translate into the nodes of these aerodynamic surfaces by terms of splines.

Beam model flutter calculations were made using quasi-static aerodynamics approach. In this approach forces are considered as dependent on the distribution of angles of attack (dynamic curvature) at a given time and don't depend on the history of movement. Also method of circulation is used at the quasi-steady approach. In the method of circulation accepted hypothesis of plane sections, not taking into account the aerodynamic interference between the sections.

It was found that it is the second eigen mode affects flutter. For air flow pressure $P = 0.6$ and Mach number $M = 0.8$ load case critical velocity for beam model is $V_{cr} = 216.5$ m/s and flutter frequency is 87.09 Hz while for FE model critical velocity is $V_{cr} = 245$ m/s and flutter frequency is 20.1 Hz.

In beam model calculation case flutter mode involve third wing bending and in FE model calculation flutter mode involve engine pitch. This is the main difference for further consideration.

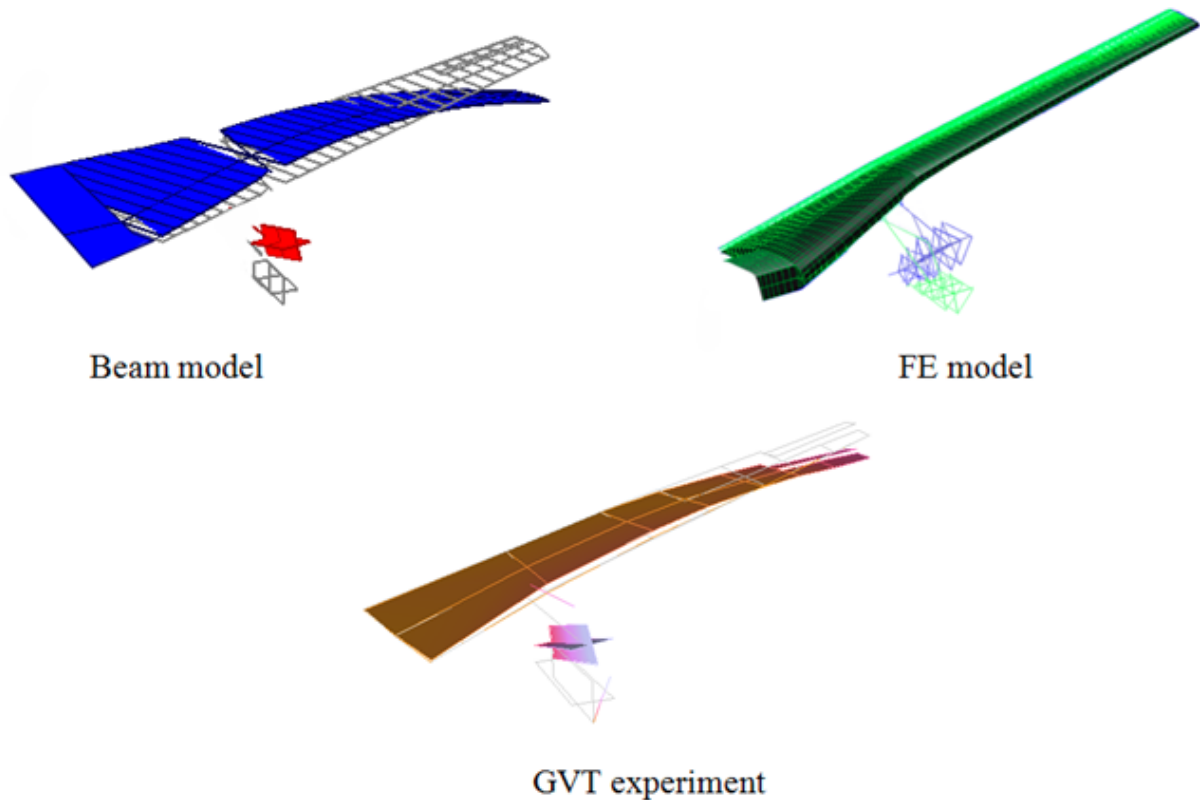


Fig. 3. Comparison of second eigenmode

2 Model manufacturing and instrumentation

During manufacturing of the model were used modern 3D-printing technology and composites. Shared use of composite materials and plastics used in 3D printing accelerated the process of model designing and creating, but complicated the task of computational research.

A large number of accelerometers and strain gauges distributed over the wing were used for measuring the dynamic characteristics. Additionally the model was equipped with special electro-hydraulic excitation device.

2.1 Model manufacturing

For modeling a high aspect ratio wing, a beam-type schematization of the full-scale structure is used. It is really very seldom that the load-bearing arrangement of the full-scale structure is reproduced on the model. This is due to the fact, that beam-type schematization offers more possibilities for carrying out

parametric studies than a structurally similar model does.

Beam-type schematization allowed providing easy access to all of the systems for checking their functionality and adjusting them, both at bench tests of the model in laboratory conditions and when carrying out the WT experiment.

Another beam-type model advantage is the fact that its strength properties are much higher than those of structurally-similar model are. The latter is critically important not only from the point of view of raising the model “survivability” in case of flutter, but also for preventing possible damage to the transonic wind tunnel compressor.

Model consists of several main parts such as caisson beam, aerodynamic contour, spring, imitating the engine pylon stiffness, engine, aileron and spring imitating the wing fuselage

stiffness.

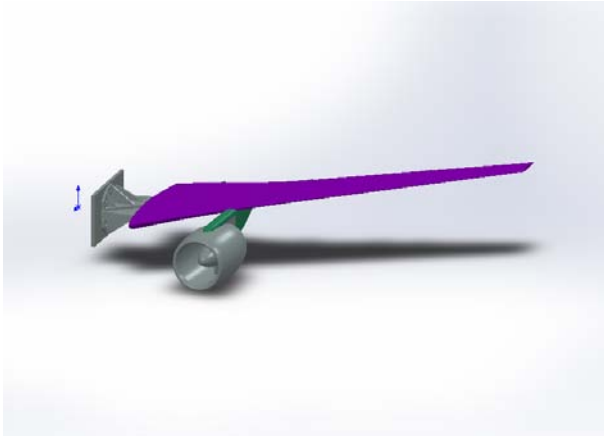


Fig. 4. Wing CAD model

The basic bearer of the model, just like in nature, is the caisson. In the model, it is a cellular girder (hollow beam) of variable cross-section spanwise, made of composite – carbon-fiber plastic. The inner, shape-generating outline of the beam is made of low-module material – polycarbonate. The specified distribution of stiffness properties spanwise is provided by the layers of high-module and high-strength unidirectional carbon-fiber plastic with layers arrangement of $[\pm 45^\circ n/0^\circ m]$ with respect to stiffness axis. To obtain the required accuracy of the beam external outline, it has been made by molding in a press mold. To fix the spring, imitating the engine pylon stiffness, special steel joint has been installed inside the beam.

Inside dynamically scaled model was installed electrohydraulic exciter.

2.2 Instrumentation

Many transducers are installed on the model: transducers specially made in TsAGI and based on ADXL of the model 326 ANALOG DEVICES (USA) with single, two-, three-axis small mass accelerometers for vibration displacement measurement (26 items); strain gauges BFLA-5-5 and FLA-5-17 made by Tokyo Sokki Kenkyujo Co., Ltd. (Japan) for relative deformations and dynamic loads measurement in polymer composit (12 items)

The subsystem is based on ADXL accelerometers modified by TsAGI of the model 326 made by Analog Devices (USA)

For accelerometers supply and matching with measurement system inputs TsAGI developed 16-channel matching repeaters (SP/16-1), line adapters for accelerometers and repeaters.

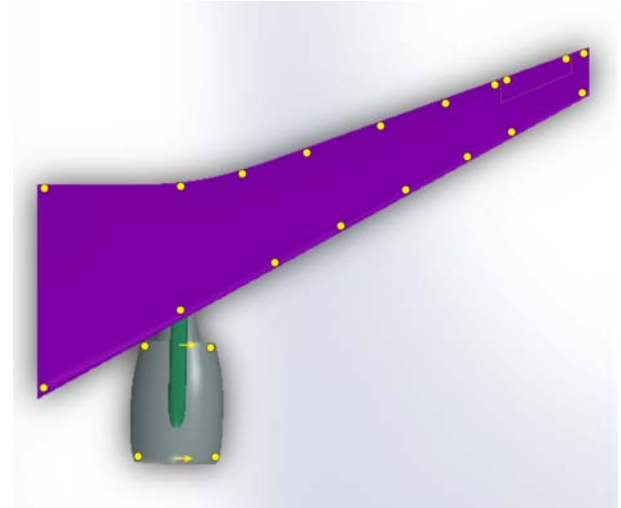


Fig. 5. Accelerometers layout

In this subsystem we used 26 accelerometers, and there were 34 vibration acceleration measurement channels taking into account two- and three-axis channels. Locations and directions of accelerometers are shown in figure 5.

We also used three 16-channels matching repeaters. Their signals were sent to the plug-board, made in the form of three 16-channels patch boards made by PCB (USA).

Strain gage subsystem is based on strain gauges BFLA-5-5 and FLA-5-17 made by Tokyo Sokki Kenkyujo Co., Ltd. On the wing box of the model made of composite there were placed half-bridge strain gauge schemes.

As strain gauge equipment in this subsystem we used 2 sets of 8-channel equipment with carrier frequency 8ANCh-26, developed by TsAGI and made by Ufa instrument-making plant.

8ANCh-26 Equipment output signals were sent to the patch board inputs, made in the form of two 8-channel panels.

Signals from the patch board were parallelly connected to data acquisition and processing systems mentioned below.

While of experimental data importance and high cost if wind tunnel time we decided to use of two measuring systems during wind

FLUTTER CALCULATIONS AND TRANSONIC WIND TUNNEL TESTING OF DYNAMICALLY SCALED MODEL

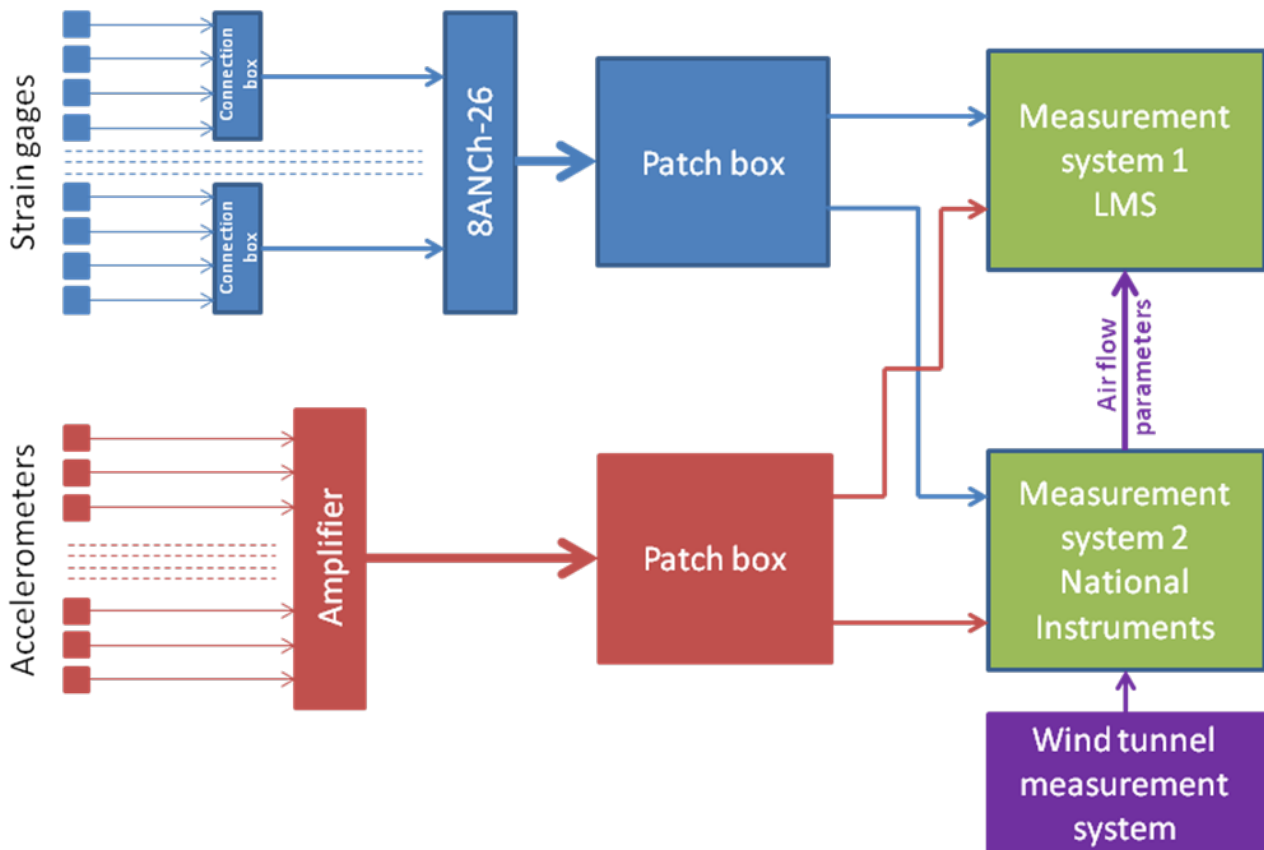


Fig. 6. Measurement systems scheme

tunnel testing. So all signals were recorded by two systems. See Fig.6.

The first system is based on LMS SCADAS III unit with V12-L programmable measurement module made by LMS International (Belgium).

The second system is based on data acquisition plate made by National Instruments. In addition auxiliary system received air flow conditions data and send to the main one as analog signals.

The first system worked with LMS Test.Lab standard program version 11B, and special software for the second system was developed by TsAGI and based on development system LabView.

- Total pressure 20–400 kPa
- Dynamic pressure up to 80 kPa
- Stagnation temperature 293–323°K
- Run duration – continuous action



Fig. 7. Wind tunnel T-128

Working section sizes are: on input 2.75 m × 2.75 m, on output 2.75 m × 3.5 m.

During runs excitation was carried out by internal exciter in two ranges from 10 to 60 Hz, and from 50 to 100 Hz, because of the most important eigenmodes was in this ranges.

2.3 Wind Tunnel Testing

Wind tunnel testing was carried out in transonic wind tunnel T-128 TsAGI.

Wind tunnel T-128 characteristics:

- Airflow Mach number range 0.15–1.7
- Re number for 1 m length up to 41·106

The model was tested in wide range of dynamic pressure and Mach numbers. Dynamic pressure was from 1000 to 2600 kgf/m, and Mach number was from 0.5 to 0.9.

During test it was accomplished continuous data acquisition. All measurement channels and airflow parameters were recorded with sampling rate 1024 Hz and stored on disk file.

The windowing used for all runs was standard for LMS system:

- Windowing – uniform;
- Spectral lines – 8196;
- Bandwidth – 520 Hz;
- FRF estimator –Hv.

During wind tunnel testing

LMS system can do standard evaluation operations (spectrums, coherence functions, transfer functions and so on). It contains also “Polymax” program to estimate eigenfrequencies, damping and eigenmodes. This program was used for data evaluation presented below. On the other hand it is necessary to note, that any identification procedure is **theoretically incorrect**. So the results of such type data evaluation are extremely sensitive to the analyst qualification, to the data involved to evaluation (type and number of transducers, data filtering, windowing) and to the evaluation procedure itself.

To overview test results LMS system can draw some useful pictures. For example waterfall pictures for selected transducer quickly show data quality, model frequencies behavior and amplitudes of vibrations

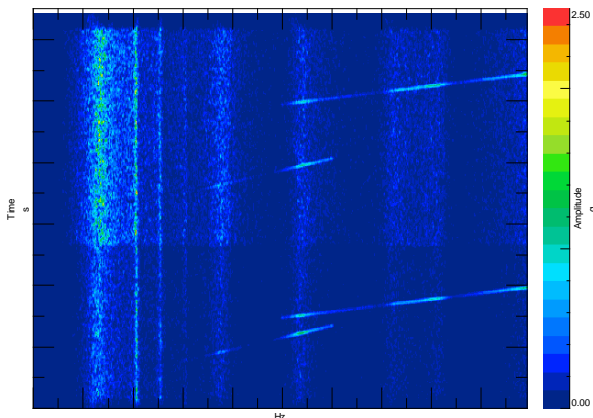


Fig. 8. Waterfall picture for accelerometer

One can see on these pictures that the run contains two regimes, that main frequencies can be detected, that excitation (sweep sine) acts on all sensors. Also it is clear, that on second regime after first frequency range was quite big delay. Maximal amplitudes are achieved when sweep sine frequency coincides with one of model eigenfrequency in the airflow.

Data evaluation was done using LMS POLYMAX option

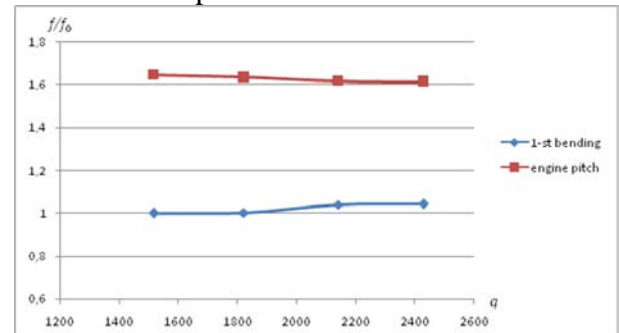


Fig. 9. First modes frequencies dependency on dynamic pressure

Typical view of dimensionless frequency (f/f_0) – dynamic pressure dependency is presented on Figure 9, damping ratios (ζ/ζ_0) – on Figure 10.

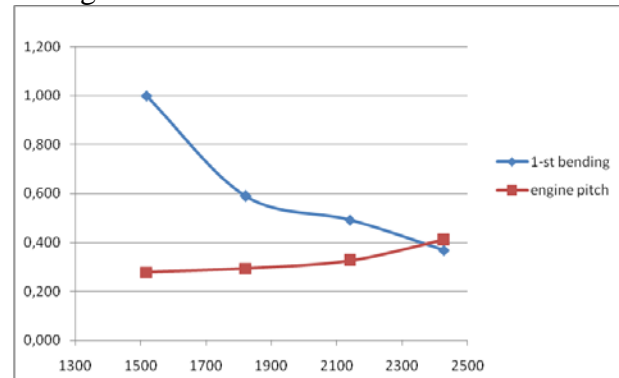


Fig. 10. First modes damping dependency on dynamic pressure

The tendency to flutter is not evident on these plots. At the same time so called Zimmerman’s “Flutter margin” (damping is not accounted for) shows that flutter boundary can exist near $Q \sim 3400 \text{ kgf/m}^2$.

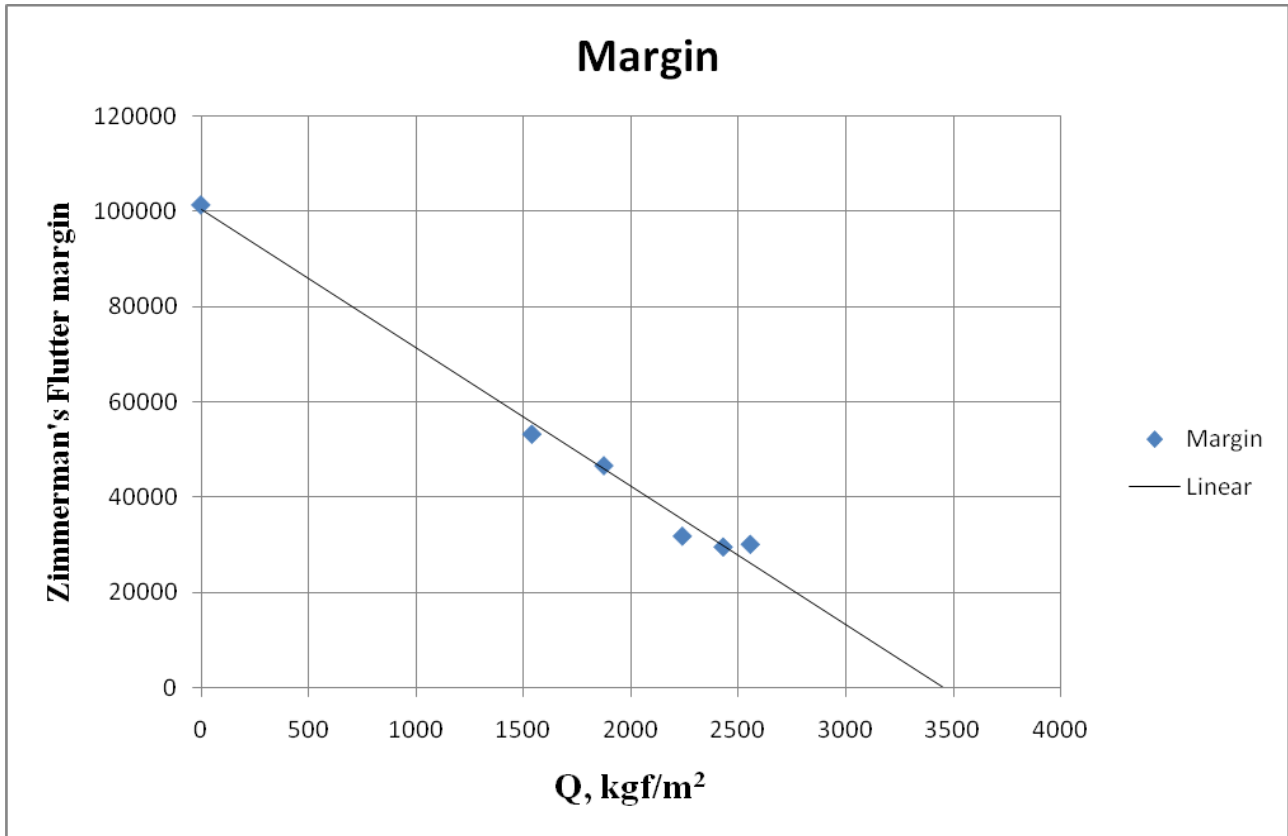


Fig. 11. Flutter margin

This is relatively far extrapolation with insufficient accuracy. FEM calculated value is about $Q \sim 4100 \text{ kgf/m}^2$. Beam model calculated value is higher $Q \sim 4800 \text{ kgf/m}^2$.

It is necessary note, that direct comparison of experimental and numerical frequencies and damping can be correct only in the case of zero damping, because aerodynamic theory is applicable only for harmonic oscillation. Only qualitative (not quantitative) comparison can be done when for example p-k method is used for flutter boundary calculation.

Conclusion

Wind tunnel tests of dynamically scaled model of high aspect ratio aircraft wing were accomplished.

Any identification procedure is theoretically incorrect. So the results of such type data evaluation are extremely sensitive to the analyst qualification, to the data involved to evaluation (type and number of transducers, data filtering, windowing) and to the evaluation procedure itself.

Direct comparison of experimental and numerical frequencies and damping can be correct only in the case of zero damping, because aerodynamic theory is applicable only for harmonic oscillation.

References

- [1] B. Peeters, H. Van der Auweraer, P. Guillaume, J. Leuridan “The PolyMAX frequency-domain method: a new standard for modal parameter estimation?”, *Shock and Vibration* 11 (2004) 395–409
- [2] Peeters, B., Karkle, P., Pronin, M., Van der Vorst, R. Operational Modal Analysis for in-line flutter assessment during wind tunnel testing. *IFASD 2011*, Paris, 2011.
- [3] LMS International.<http://www.lmsintl.com/>
- [4] ZIMMERMAN, N.H., WEISSENBURGER, J.T. Prediction of flutter onset speed based on flight testing at subcritical speeds. *Journal of Aircraft*, 1(4):190-202, 1964

Contact Author Email Address

Contact Author: Mikhail Pronin
mailto: mikhail.pronin@tsagi.ru

Copyright Statement

The authors confirm that they, and/or their company or organization, hold copyright on all of the original material included in this paper. The authors also confirm that they have obtained permission, from the copyright holder of any third party material included in this paper, to publish it as part of their paper. The authors confirm that they give permission, or have obtained permission from the copyright holder of this paper, for the publication and distribution of this paper as part of the ICAS 2014 proceedings or as individual off-prints from the proceedings.